

Kinetic Investigations of the Rate-Limiting Step in Human 12- and 15-Lipoxygenase[†]

Erika N. Segraves and Theodore R. Holman*

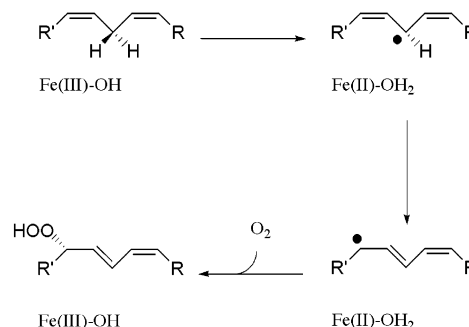
Department of Chemistry and Biochemistry, University of California, Santa Cruz, California 95064

Received December 11, 2002; Revised Manuscript Received March 21, 2003

ABSTRACT: Mammalian lipoxygenases have been implicated in several inflammatory disorders; however, the details of the kinetic mechanism are still not well understood. In this paper, human platelet 12-lipoxygenase (12-hLO) and human reticulocyte 15-lipoxygenase-1 (15-hLO) were tested with arachidonic acid (AA) and linoleic acid (LA), respectively, under a variety of changing experimental conditions, such as temperature, dissolved oxygen concentration, and viscosity. The data that are presented show that 12-hLO and 15-hLO have slower rates of product release (k_{cat}) than soybean lipoxygenase-1 (sLO-1), but similar or better rates of substrate capture for the fatty acid ($k_{\text{cat}}/K_{\text{M}}$) or molecular oxygen [$k_{\text{cat}}/K_{\text{M}(\text{O}_2)}$]. The primary, kinetic isotope effect (KIE) for 15-hLO with LA was determined to be temperature-independent and large ($^{\text{D}}k_{\text{cat}} = 40 \pm 8$), over the range of 10–35 °C, indicating that C–H bond cleavage is the sole rate-limiting step and proceeds through a tunneling mechanism. The $^{\text{D}}k_{\text{cat}}/K_{\text{M}}$ for 15-hLO, however, was temperature-dependent, consistent with our previous results [Lewis, E. R., Johansen, E., and Holman, T. R. (1999) *J. Am. Chem. Soc.* 121, 1395–1396], indicating multiple rate-limiting steps. This was confirmed by a temperature-dependent, $k_{\text{cat}}/K_{\text{M}}$ solvent isotope effect (SIE), which indicated a hydrogen bond rearrangement step at low temperatures, similar to that of sLO-1 [Glickman, M. H., and Klinman, J. P. (1995) *Biochemistry* 34, 14077–14092]. The KIE could not be determined for 12-hLO due to its inability to efficiently catalyze LA, but the $k_{\text{cat}}/K_{\text{M}}$ SIE was temperature-independent, indicating distinct rate-limiting steps from both 15-hLO and sLO-1.

Lipoxygenases are found in a large variety of organisms, such as bacteria (1), plants (2, 3), and mammals (4). In plants, lipoxygenase is involved in germination and senescence (5, 6). In humans, the products of lipoxygenase are the precursors to leukotrienes and lipoxins, which have been implicated as critical signaling molecules in a variety of inflammatory diseases and cancers (7–10). Human 5-lipoxygenase is implicated in bronchial constriction (11) and prostate cancer (12) and 12-lipoxygenase in immune disorders (13) and breast cancer (14, 15), while 15-lipoxygenase is implicated in the primary stage of atherosclerosis (16) and colorectal cancer (17). The importance of these enzymes in inflamma-

Scheme 1



tion and cancer regulation has elicited great interest in human lipoxygenase as a potential therapeutic target and emphasizes the need for further investigations of the lipoxygenase mechanism.

Historically, soybean lipoxygenase-1 (sLO-1)¹ has been the most extensively studied enzyme of all the lipoxygenases due to its ease of purification and kinetic stability. Investigators have determined that sLO-1 activates the 1,4-diene portion of linoleic acid (LA) for attack by molecular oxygen to produce the hydroperoxide product, 13(*S*)-hydroperoxy-9(*Z*),11(*E*)-octadecadienoic acid (HPOD) (Scheme 1) (3, 18). The molecular mechanism of this reaction entails activation of the resting Fe(II)–OH₂ enzyme by 1 equiv of HPOD to produce the active Fe(III)–OH species (19, 20). The Fe(III)–OH species then stereospecifically abstracts the *pro-S* hydrogen atom through a tunneling mechanism, leaving a pentadienyl radical (21–23). The mechanism of this abstrac-

[†] This research was supported by grants from the National Institutes of Health (GM56062-01).

* To whom correspondence should be addressed. E-mail: tholman@chemistry.ucsc.edu. Phone: (831) 459-5884. Fax: (831) 459-2935.

¹ Abbreviations: AA, arachidonic acid [eicosa-5(*Z*),8(*Z*),11(*Z*),14(*Z*)-tetraenoic acid]; LA, linoleic acid [9(*Z*),12(*Z*)-octadecadienoic acid]; D-LA, perdeuterated linoleic acid; HPOD, 13(*S*)-hydroperoxy-9(*Z*),11(*E*)-octadecadienoic acid; ICP-MS, inductively coupled plasma mass spectroscopy; MCD, magnetic circular dichroism; RP-HPLC, reverse phase HPLC; SDS–PAGE, sodium dodecyl sulfate–polyacrylamide gel electrophoresis; LO, lipoxygenase; 12-hLO, human platelet 12-lipoxygenase; 15-hLO, human reticulocyte 15-lipoxygenase-1; 15-rLO, rabbit reticulocyte 15-lipoxygenase; sLO, soybean lipoxygenase; k_{cat} , enzymatic first-order rate constant for fatty acid substrate; $k_{\text{cat}}/K_{\text{M}}$, enzymatic second-order rate constant for fatty acid substrate; $k_{\text{cat}}/K_{\text{M}(\text{O}_2)}$, enzymatic second-order rate constant for molecular oxygen substrate; noncompetitive KIE, kinetic isotope effect determined by using pure protio and pure deuterio substrate in steady-state kinetics; $^{\text{D}}k_{\text{cat}}$, kinetic $k_{\text{H}}/k_{\text{D}}$ isotope effect on k_{cat} ; $^{\text{D}}k_{\text{cat}}/K_{\text{M}}$, kinetic $k_{\text{H}}/k_{\text{D}}$ isotope effect on $k_{\text{cat}}/K_{\text{M}}$; SIE, solvent isotope effect.

tion has recently been postulated to proceed through an environmentally coupled mechanism where both position and molecular motion dictate the hydrogen atom abstraction (24). Molecular oxygen then regio- and stereospecifically attacks the (*S*)-face of the radical via a hydrophobic pocket in the active site (25), creating a hydroperoxide radical, which is subsequently reduced to HPOD. The microscopic rate-limiting steps for substrate capture (k_{cat}/K_M) by sLO-1 at 5 °C have been determined to be diffusion, hydrogen bond rearrangement, and hydrogen atom abstraction (26). [The terms substrate capture (k_{cat}/K_M) and product release (k_{cat}) have been defined previously (27) and shall be used in the same manner in this report.] Our lab has proposed that the hydrogen bond rearrangement step is due to the hydrogen bond network (Gln₄₉₅, Gln₆₉₇, and Asn₆₉₄) that connects the substrate cavity (Gln₄₉₅) to the iron atom (Asn₆₉₄), potentially triggering a change in the iron environment and its reactivity (23). As the temperature increases, however, the abstraction step becomes the sole rate-limiting step for substrate capture. The rate of product release (k_{cat}) for sLO-1, however, has been shown to be solely dependent on hydrogen atom abstraction, from 5 to 40 °C (28).

The mammalian enzymes are similar to plant lipoygenases with regard to their sequence homologies and structure, as seen by comparing the soybean lipoyxygenase structures with the rabbit reticulocyte 15-lipoyxygenase (15-rLO) structure (29–35). However, little is known regarding the molecular mechanism by which the mammalian lipoygenases generate the hydroperoxide product from arachidonic acid (AA). This is primarily due to their difficulty in purification and their rapid auto-inactivation, which makes steady-state kinetics difficult to interpret. We circumvented these complications with human reticulocyte 15-lipoyxygenase-1 (15-hLO) by using a competitive kinetic isotope effect (KIE) method, in which a mixture of protio- and deuterio-LA was utilized as the substrate, determining that 15-hLO abstracts the hydrogen atom through a tunneling mechanism and has a $^Dk_{\text{cat}}/K_M$ of 47 ± 7 at 5 μM substrate (36). In addition, we determined that the $^Dk_{\text{cat}}/K_M$ was temperature-dependent, indicating multiple rate-limiting steps at low temperatures, as for sLO-1. This was an intriguing result because 15-hLO has significantly lower rates of product release (k_{cat}) than sLO-1. Previously, we postulated that this lowered rate for 15-hLO was due to an increase in the ligand sphere strength of the active site iron (His₅₄₄ ligand for 15-hLO vs Asn₆₉₄ ligand for sLO-1), which would lower the driving force of the hydrogen atom abstraction and hence lower k_{cat} (37). One could then speculate that a slower k_{cat} would create a kinetic bottleneck and make hydrogen atom abstraction the sole rate-limiting step of both substrate capture (k_{cat}/K_M) and product release (k_{cat}) for 15-hLO; however, this is not the case. 15-hLO manifests multiple rate-limiting steps for substrate capture, despite a lowered rate of hydrogen atom abstraction. In this paper, we have extended this investigation to include steady-state kinetic studies of 15-hLO and human platelet 12-lipoyxygenase (12-hLO), to determine the nature of the multiple rate-limiting steps and compare their mechanisms with that of sLO-1.

MATERIALS AND METHODS

Materials. LA and AA were purchased from Aldrich Chemical Co., and perdeuterated linoleic acid (D-LA) was

purified from a mixture of perdeuterated algal fatty acids from Cambridge Isotope Labs, as previously described (38). All other reagents were reagent grade or better and were used without further purification.

RP-HPLC Purification of AA, LA, and D-LA. All commercial fatty acids were repurified using a Higgins Analytical Haisil (25 cm \times 4.6 mm) C-18 column. Solution A was 99.9% MeOH and 0.1% acetic acid, while solution B was 99.9% H₂O and 0.1% acetic acid. An isocratic elution of 85% A and 15% B was used to purify all commercial fatty acids, and they were stored at -80 °C for a maximum of 6 months.

Expression and Purification of Lipoyxygenases. 12-hLO and 15-hLO were expressed and purified as described previously (39). Briefly, both enzymes contain His tags and must be purified in one step, and then stored in glycerol at -80 °C, or significant inactivation occurs. The iron contents of all lipoyxygenase enzymes were determined on a Finnegan inductively coupled plasma mass spectrometer (ICP-MS), using internal standards of cobalt(II)-EDTA, and data were compared with those of standardized iron solutions. All kinetic measurements were standardized to iron content.

Steady-State Kinetic Measurements. Steady-state kinetic values were determined by following the formation of the conjugated product at 234 nm ($\epsilon = 2.5 \times 10^4 \text{ M}^{-1} \text{ cm}^{-1}$) with a Perkin-Elmer Lambda 40 spectrophotometer. No photodegradation of the product was observed. Assays of 12-hLO were carried out in 25 mM Trizma buffer (pH 7.5), and assays of 15-hLO were carried out in 25 mM Hepes buffer (pH 7.5). LA and AA concentrated stock solutions were stored in 95% ethanol, and diluted into buffer so that the total ethanol concentration was less than 1.5%. Fatty acid concentrations were verified by allowing the enzyme reaction to proceed to completion, and quantitating at 234 nm. Enzymatic reactions were initiated by the addition of ≈ 5 nM 12-hLO or ≈ 30 nM 15-hLO (normalized to iron content). Assays were 2 mL in volume with substrate concentrations ranging from 1 to 25 μM and were constantly stirred with a rotating magnetic bar. It should be noted that higher substrate concentrations were avoided to prevent the formation of micelles, which would alter the free substrate concentration (40). Initial rates (up to the first 15% of the reaction) for each substrate were fitted to the Michaelis–Menten equation using the KaleidaGraph (Synergy) program on a Macintosh and errors determined. All subsequent kinetic measurements were handled in a similar form.

pH Studies. Kinetic measurements were determined over a pH range of 7–9 in Trizma and Hepes buffer. The total ionic strength was adjusted in all cases to 25 mM by the addition of NaCl. Hepes buffer was found to inhibit 12-hLO but not 15-hLO; consequently, further kinetic studies were performed using Trizma with 12-hLO and Hepes with 15-hLO.

Temperature Dependence. Initial rates of reaction were measured by the above methods. Temperature control of the reaction was achieved by using temperature-controlled cuvettes with a stream of nitrogen gas to inhibit condensation. To account for temperature-induced pH differences in Trizma and Hepes, buffers were equilibrated to temperatures from 10 to 45 °C and then the pHs adjusted.

Reaction Rates at Varying O₂ Concentrations. Reaction rates of 12-hLO (AA) and 15-hLO (LA) were determined

by measuring the extent of oxygen consumption on a Clark oxygen monitor as previously described (26). Reactions were carried out as a function of oxygen concentration in 1 mL solutions, which were constantly stirred and equilibrated under air at 25 °C (258 μM O_2). The reaction was initiated by addition of ≈ 10 nM 12-hLO and ≈ 30 nM 15-hLO (normalized to iron content) via a gastight Hamilton syringe to the reaction chamber. The experiments were repeated at a number of different concentrations of oxygen established by passing mixtures of N_2 and O_2 over stirred solutions in the reaction chamber for 20 min. The new oxygen concentration was calibrated against the value of O_2 dissolved in an air-saturated solution at 25 °C (258 μM O_2). The rate of oxygen consumption was recorded at O_2 concentrations from 300 to 5 μM . The fatty acid substrate concentration was 5 times the K_M for the respective enzyme, 15 μM AA for 12-hLO and 25 μM LA for 15-hLO.

Kinetic Isotope Effects. The KIE values were determined by comparing steady-state results using pure protio-LA and pure perdeuterated LA (D-LA) substrates and should be differentiated from competitive KIE values where there is a mixture of proteo and deuterio substrate in the reaction flask. Steady-state KIE values were determined for 15-hLO by following the formation of the conjugated product at 234 nm, as discussed above, and were carried out in 25 mM Hepes buffer (pH 7.5). For protonated LA, ≈ 45 nM 15-hLO was used for each assay and ≈ 105 nM 15-hLO (normalized to iron content) to determine the D-LA kinetics.

Solvent Isotope Effects. Kinetic measurements were performed with 12-hLO and 15-hLO at temperatures from 10 to 45 °C in 25 mM buffer (Trizma and Hepes, respectively) using H_2O or D_2O , pL 7.5 (the pH meter reading was 7.1 for D_2O). SIE results were determined by averaging the values from three separate experiments. Since the LA has a pK_a value between 7 and 8 in buffer solutions not containing detergent (26), the influence of pH on our SIE experiments with 15-hLO in 25 mM Hepes was also examined at pL 7.1, 7.5, and 7.9.

Viscosity Studies. Reactions were carried out at different relative viscosities ($\eta_{\text{rel}} = \eta/\eta^0$, where η^0 is the viscosity of H_2O at 20 °C) to determine if the human lipoxygenase catalysis is diffusion-controlled. A number of viscogens were surveyed (ethylene glycol, glycerol, dextrose, maltose, and sucrose) by adding 1 mL of viscogen at varying concentrations to 1 mL of substrate buffer solution ($2 \times$ concentration) and monitored as discussed previously for the steady-state kinetics.

RESULTS

Expression and Purification of Lipoxygenases. Both 12-hLO and 15-hLO yielded approximately 50 mg/L from the one-step, His-Bind (Qiagen) column and were greater than 90% pure, as judged by SDS-PAGE (stained with Coomassie brilliant blue, data not shown). As isolated, ICP-MS indicated that the human enzymes contained 0.35 mol of iron per mole enzyme, on average, and all kinetic values were corrected for iron content.

pH Studies. Changing the pH of the buffer while maintaining a constant ionic strength revealed that 12-hLO and 15-hLO exhibited their highest activities in the pH range of 7–8 (data not shown), consistent with previous results for 12-

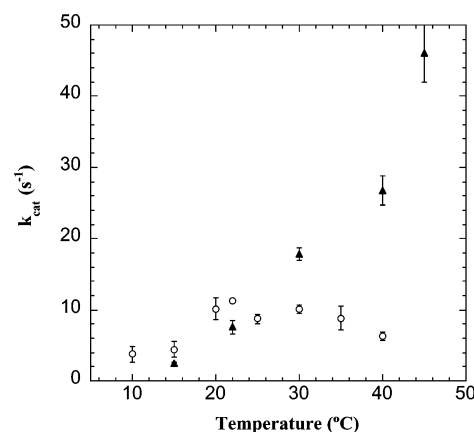


FIGURE 1: Temperature dependence of the observed k_{cat} of 12-hLO (\blacktriangle) and 15-hLO (\circ) in the temperature range of 10–45 °C at pH 7.5.

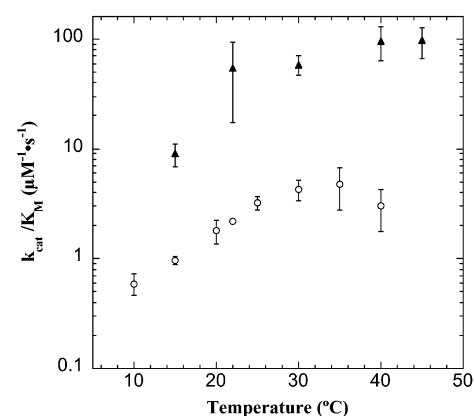


FIGURE 2: Temperature dependence of the observed k_{cat}/K_M of 12-hLO (\blacktriangle) and 15-hLO (\circ) in the temperature range of 10–45 °C at pH 7.5. Because of the difference of more than 1 order of magnitude between the k_{cat}/K_M values of 12-hLO and 15-hLO, the y-axis is displayed as logarithmic.

Table 1: Comparison of Kinetic Parameters for sLO-1,^a 12-hLO,^b and 15-hLO^c

	k_{cat}^d (s^{-1})	k_{cat}/K_M^d ($\mu\text{M}^{-1} \text{s}^{-1}$)	$k_{\text{cat}}/K_{M(\text{O}_2)}^e$ ($\mu\text{M}^{-1} \text{s}^{-1}$)
sLO-1	297 (12) ^f	11 (1) ^f	4.4 (0.6) ^g
12-hLO	17.8 (0.8)	59 (12)	1.9 (0.4)
15-hLO	10.1 (0.6)	4.3 (0.9)	1.3 (0.3)

^a Data were collected in borate buffer (pH 9.0) with LA. ^b Data were collected in Tris buffer (pH 7.5) with AA. ^c Data were collected in Hepes buffer (pH 7.5) with LA. ^d The rate constants (k_{cat} and k_{cat}/K_M) are reported for 30 °C. ^e The rate constants [$k_{\text{cat}}/K_{M(\text{O}_2)}$] are reported for 20 °C. ^f From ref 24. ^g From ref 25.

hLO (41). Therefore, all further kinetic experiments were performed at physiological pH (7.5).

Kinetic Analysis of 12-hLO and 15-hLO. Both human lipoxygenases exhibited hyperbolic steady-state kinetics from which the rate constants k_{cat} (Figure 1) and k_{cat}/K_M (Figure 2) were determined (Table 1). It should be noted that severe autoinactivation was observed at high substrate concentrations for both enzymes if the substrate was not HPLC-purified and stored at -80 °C. This suggests that the reaction products of substrate oxidation by molecular oxygen may lead to autoinactivation of human lipoxygenases. 12-hLO displayed an increasing k_{cat} value, from $2.5 \pm 0.1 \text{ s}^{-1}$ at 15 °C to $46 \pm 4 \text{ s}^{-1}$ at the maximum temperature that was tested,

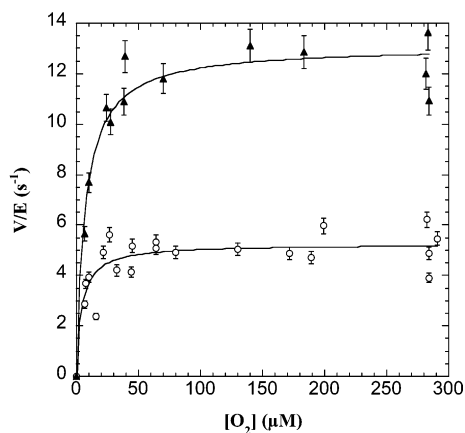


FIGURE 3: Initial rates of 12-hLO (\blacktriangle) and 15-hLO (\circ) as a function of oxygen concentration with saturating fatty acid substrate (20 °C and pH 7.5). Rates of oxygen consumption were determined as described in Materials and Methods and were defined as micromoles of dioxygen consumed per micromole of lipoxygenase per second (V/E). Data were fit to the Michaelis–Menten equation.

45 °C. These values were higher than those previously recorded, most likely due to our correction for iron content (41). For 15-hLO, the k_{cat} value of $10.2 \pm 1.6 \text{ s}^{-1}$ (20 °C) agreed with our previously reported results for 15-hLO without a His tag and demonstrates the His tag has no effect on catalysis (40). 15-hLO showed a maximum velocity between 20 and 35 °C, which then decreased with increasing temperature. To investigate this decrease in k_{cat} for 15-hLO at higher temperatures, we performed a series of experiments to evaluate autoinactivation of both human lipoxygenases at 15, 30, and 45 °C. We added three sequential additions of HPLC-purified substrate to the enzyme and compared their rates as the reaction was allowed to go to completion (data not shown). These experiments indicated that 15-hLO underwent autoinactivation with increasing temperature and thus lowered the k_{cat} for 15-hLO, consistent with previous results (42, 43). 12-hLO was not observed to experience a decrease in rate, but rather, the k_{cat} increased at high temperatures, indicating little autoinactivation with HPLC-purified AA. The $k_{\text{cat}}/K_{\text{M}}$ value (Figure 2) for both enzymes increased with increasing temperature and leveled off above 30 °C (average value above 30 °C for 12-hLO of $96.2 \pm 0.5 \mu\text{M}^{-1} \text{ s}^{-1}$ and for 15-hLO $3.9 \pm 1.2 \mu\text{M}^{-1} \text{ s}^{-1}$).

Reaction Rates at Varying O_2 Concentrations. The kinetic parameters for both enzymes were analyzed under saturating fatty acid substrate conditions ($5K_{\text{M}}$) at 20 °C (Figure 3). The $K_{\text{M}(\text{O}_2)}$ was determined to be 7.0 ± 1.4 and $4.2 \pm 1.1 \mu\text{M}$ for 12-hLO and 15-hLO, respectively (the lowest attainable concentration of O_2 was $5 \mu\text{M}$, which leads to a large uncertainty in both of these K_{M} determinations). The k_{cat} was determined to be $13.1 \pm 0.4 \text{ s}^{-1}$ for 12-hLO and $5.2 \pm 0.2 \text{ s}^{-1}$ for 15-hLO, which are in good agreement with k_{cat} values determined spectrophotometrically. A similar correspondence between k_{cat} values determined spectrophotometrically and by the Clarke electrode has previously been reported for sLO-1 (22).

Kinetic Isotope Effect. Previously, we reported a large $^{\text{D}}k_{\text{cat}}/K_{\text{M}}$ result at $5 \mu\text{M}$ LA/D-LA for 15-hLO using a competitive HPLC method (36). We expanded these results by using a noncompetitive KIE method, previously devised by Klinman and co-workers for sLO-1, in which steady-state kinetics were performed with pure LA and pure D-LA, separately

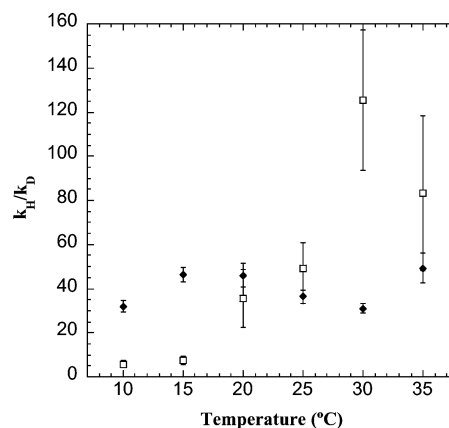


FIGURE 4: Temperature dependence of the apparent primary $k_{\text{H}}/k_{\text{D}}$ for 15-hLO at pH 7.5: $^{\text{D}}k_{\text{cat}}$ (\blacklozenge) and $^{\text{D}}k_{\text{cat}}/K_{\text{M}}$ (\square).

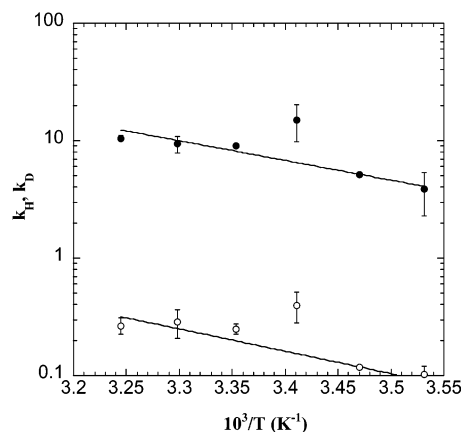


FIGURE 5: Arrhenius plot of kinetic data for 15-hLO using protiolinoleic acid (\bullet) and deuteriolinoleic acid (\circ). Nonlinear fits to the Arrhenius equation are shown as solid lines.

(44). LA and D-LA were used because the appropriately deuterated AA was not available. LA as a substrate was comparable to AA for 15-hLO (45); however, 12-hLO was only 4% as active with LA as with AA (41). Consequently, KIE experiments were undertaken with only 15-hLO (Figure 4). The $^{\text{D}}k_{\text{cat}}$ value for 15-hLO was largely temperature independent over the experimental range from 10 to 35 °C ($^{\text{D}}k_{\text{cat}} = 40 \pm 8$). This KIE result was much larger than semiclassical theory predicts ($\text{KIE} = 7\text{--}10$) and was consistent with a tunneling mechanism for hydrogen atom abstraction (46). The temperature independence of $^{\text{D}}k_{\text{cat}}$ indicated that the product release was fully rate limited by hydrogen atom abstraction. $^{\text{D}}k_{\text{cat}}/K_{\text{M}}$, however, was not temperature-independent and increased with increasing temperature to 83 ± 35 (35 °C). It should be noted that the $^{\text{D}}k_{\text{cat}}/K_{\text{M}}$ values at 30 and 35 °C have extremely high error values because the calculated K_{m} values from the LA and D-LA steady-state kinetics have high errors and thus the calculated KIE error values are high. This high error in K_{m} is most likely due to the large degree of autoinactivation at these temperatures for 15-hLO.

The temperature dependences of $^{\text{D}}k_{\text{cat}}$ (Figure 5) for both hydrogen and deuterium atom abstraction were fitted with the empirical Arrhenius equation ($k = A \exp^{-E_{\text{act}}/RT}$), where R represents the gas constant, T is the absolute temperature, E_{act} is the activation energy, and A is the Arrhenius prefactor (Table 2). 15-hLO exhibits a weak temperature dependence ($E_{\text{act}} = 7.7 \text{ kcal/mol}$) and a moderate Arrhenius prefactor

Table 2: Energy of Activation and Arrhenius Prefactor Isotope Effects for sLO-1^a and 15-hLO^b

	k_{cat}^c (s ⁻¹)	KIE ^d	E_{act} (kcal/mol)	ΔE_{act}^e (kcal/mol)	A_{H} (s ⁻¹)	$A_{\text{H}}/A_{\text{D}}$
sLO-1 ^f	297 (12)	81 (5)	2.1 (0.2)	0.9 (0.2)	9×10^3 (2×10^3)	18 (5)
15-hLO	10.1 (0.6)	40 (8)	7.7 (0.3)	1.0 (0.1)	3×10^6 (2×10^6)	8 (14)

^a Data were collected between 5 and 50 °C in borate buffer (pH 9.0). ^b Data were collected between 10 and 35 °C in Hepes buffer (pH 7.5). ^c The rate constant (k_{cat}) is reported for 30 °C. ^d $\text{KIE} = {}^Dk_{\text{cat}} = k_{\text{cat}}^{\text{H}}/k_{\text{cat}}^{\text{D}}$. ^e This is the isotope effect on E_{act} ($\Delta E_{\text{act}} = E_{\text{act}}^{\text{D}} - E_{\text{act}}^{\text{H}}$). ^f From ref 24.

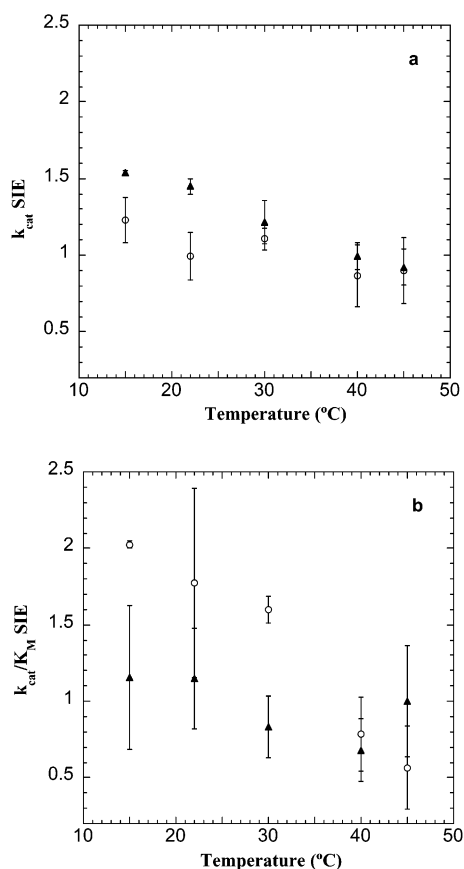


FIGURE 6: Solvent isotope effects for the lipoxigenase reaction. Temperature dependence of the observed k_{cat} (a) and $k_{\text{cat}}/K_{\text{M}}$ (b) of 12-hLO (▲) and 15-hLO (○) in the range of 15–45 °C at pH 7.5.

($A_{\text{H}} \approx 3 \times 10^6$ s⁻¹) with LA. Additionally, the ΔE_{act} is near unity (ΔE_{act} is the difference between the protio and deuterio E_{act} values), and the KIE is close to being temperature-independent, leading to an $A_{\text{H}}/A_{\text{D}}$ value of >1 (8 ± 14). The large degree of error makes the $A_{\text{H}}/A_{\text{D}}$ value difficult to interpret.

Solvent Isotope Effects. The kinetic parameters k_{cat} (Figure 6a) and $k_{\text{cat}}/K_{\text{M}}$ (Figure 6b) for both lipoxigenases were analyzed with substrate in H₂O or D₂O over the temperature range of 10–45 °C. The k_{cat} SIE for 12-hLO was 1.5 ± 0.01 , indicating a solvent-dependent step that was partially rate-limiting at 15 °C. As the temperature was increased, the k_{cat} SIE for 12-hLO decreased to unity, indicating no rate-limiting solvent-dependent steps at higher temperatures. The k_{cat} SIE for 15-hLO, however, was temperature-independent (1.0 ± 0.2 , average value from 15 to 45 °C), which indicated no solvent-dependent rate-limiting steps for product release. The $k_{\text{cat}}/K_{\text{M}}$ SIE for 12-hLO was temperature-independent (1.0 ± 0.2 , average value from 15 to 45 °C), while the value for 15-hLO was 2.0 ± 0.02 (15 °C) and was temperature-dependent. The temperature dependence of the $k_{\text{cat}}/K_{\text{M}}$ SIE for 15-hLO indicated that there was a solvent-dependent step

that was partially rate-limiting at low temperatures and not rate-limiting above 30 °C. These interpretations were tempered by the relatively large error values for these reactions, because of the imprecise nature of K_{M} . This higher error was most likely due to the previously mentioned autoinactivation and the fact that high concentrations of substrate can lead to substrate inhibition for the human lipoxigenases (40). The SIE for 15-hLO was also monitored for a pH effect and found to be constant in the pH range of 7.1–7.9 (data not shown).

Viscosity Studies. Viscosity experiments were attempted with ethylene glycol, dextrose, sucrose, maltose, and glycerol to test diffusion; however, no two viscogens produced comparable viscosity dependence for either 12-hLO or 15-hLO, and therefore, no conclusions could be drawn.

DISCUSSION

In this paper, we investigated the kinetic mechanism of both 15-hLO and 12-hLO utilizing a variety of steady-state kinetic methods to compare their properties directly with those of the well-studied sLO-1 enzyme. The steady-state data obtained by varying the fatty acid substrate concentration demonstrated that the rate of product release (k_{cat}) for both 12-hLO and 15-hLO is significantly slower at 30 °C than that of sLO-1, 17- and 29-fold, respectively (Table 1). The rate of substrate capture ($k_{\text{cat}}/K_{\text{M}}$), however, is more comparable to that of sLO-1, with 15-hLO being 3-fold slower and 12-hLO being 5-fold faster at 30 °C. The $k_{\text{cat}}/K_{\text{M}}$ values are comparable among the three enzymes as a consequence of lowered K_{M} values for the human enzymes (where $K_{\text{M}} = 0.30 \pm 0.06$ μM for 12-hLO, $K_{\text{M}} = 2.4 \pm 0.5$ μM for 15-hLO, and $K_{\text{M}} = 27$ μM for sLO-1) (25), potentially indicating reduced dissociation constants for the human enzymes with the fatty acid substrate. The temperature effect on these kinetic parameters shows that the k_{cat} of 15-hLO is diminished at temperatures higher than 37 °C, while the k_{cat} of 12-hLO increases monotonically, up to 45 °C (Figure 1). The decrease in k_{cat} at higher temperatures for 15-hLO was due to the autoinactivation at high substrate concentrations, as seen in this paper and in other studies (42, 43, 47, 48). The $k_{\text{cat}}/K_{\text{M}}$ values for both 12-hLO and 15-hLO plateau above 30 °C, which coincides with the physiological temperature (37 °C) for both human enzymes (Figure 2). The rate of oxygen incorporation (Figure 3 and Table 1) shows that the $k_{\text{cat}}/K_{\text{M}(\text{O}_2)}$ for the human enzymes is only 2–3-fold less than that for sLO-1, which can be attributed to the $K_{\text{M}(\text{O}_2)}$ values for 12-hLO (7.0 ± 1.4 $\mu\text{M O}_2$) and 15-hLO (4.2 ± 1.1 $\mu\text{M O}_2$) that are lower than that of sLO-1 (48 $\mu\text{M O}_2$) (25). This is significant to their biological activity since the dissolved O_2 concentration in tissue has been reported to be between 10 and 40 μM (49), and therefore, the $K_{\text{M}(\text{O}_2)}$ values for 12-hLO and 15-hLO are sufficiently low that dissolved oxygen is saturating. These combined kinetic data suggest that the human enzymes have evolved such that their overall

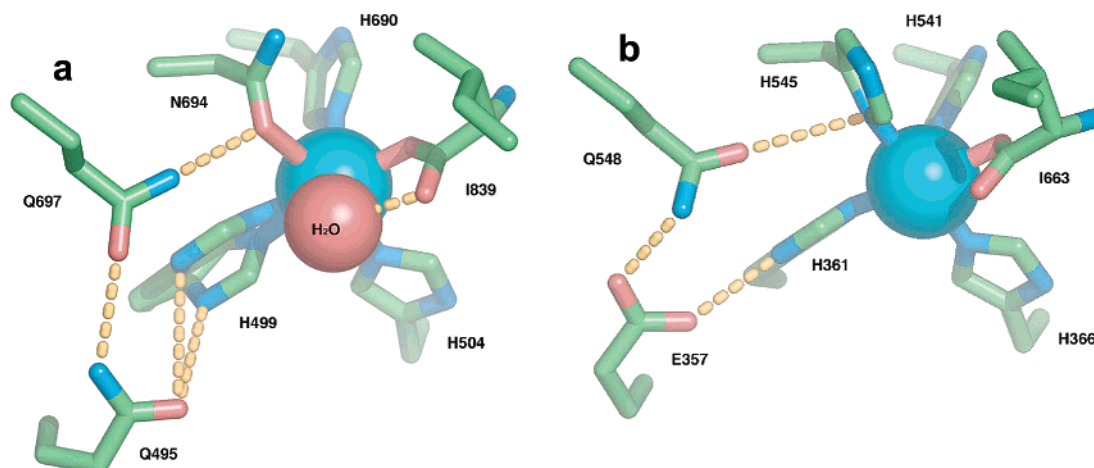


FIGURE 7: View of the hydrogen bond network of wild-type sLO-1 (a) and 15-rLO (b). The iron atom is colored cyan, and the residues that form the hydrogen bond network are connected by yellow, dashed bonds. H₄₉₉ of sLO-1 was found to be in two conformations of approximately equal proportions, and the water in the 15-rLO structure is not present, presumably due to its exclusion from the active site by the bound inhibitor (permission to reproduce figure granted by M. Browner).

turnover rate (i.e., k_{cat}) has decreased significantly relative to that of sLO-1, but their ability to initiate the reaction [i.e., $k_{\text{cat}}/K_{\text{M}}$ and $k_{\text{cat}}/K_{\text{M(O}_2\text{)}}$] is comparable to or better than that of sLO-1. This point is significant as $k_{\text{cat}}/K_{\text{M}}$ is generally considered to represent the rate constant under physiological conditions and suggests that both human enzymes are optimized as physiological catalysts (50).

The differences in the general kinetic properties of the three lipoxygenases lead us to investigate the nature of the rate-limiting steps for both 12-hLO and 15-hLO and determine how the human enzymes are different from sLO-1 on a microscopic kinetic level. 12-hLO is difficult to study by primary kinetic isotope effects because LA is not a substrate and appropriately deuterated AA is not commercially available. Viscosity dependence could also not be determined because the viscogens that were tested gave varying results. The only isotopic experiment available was that of comparing kinetic rates in H₂O and D₂O (Figure 6). To this end, we observe that k_{cat} was solvent-dependent at low temperatures, while $k_{\text{cat}}/K_{\text{M}}$ is solvent-independent between 10 and 40 °C. This is in sharp contrast to sLO-1, for which k_{cat} is solvent-independent at all temperatures but $k_{\text{cat}}/K_{\text{M}}$ is solvent-dependent at low temperatures. These results indicate a fundamental change in the microscopic rate constants between the two enzymes; however, its origin is difficult to determine without primary KIE results. Interestingly, sequence analysis with 12-hLO and sLO-1 suggests that they have very similar iron coordination environments: both 12-hLO and sLO-1 have Asn as the sixth ligand, which would imply similar reduction potentials (i.e., similar abstraction chemistry). This, coupled with the fact that 12-hLO has a greater kinetic turnover rate than 15-hLO, suggests that 12-hLO should have a mechanism similar to that of sLO-1, but this is not the case. We are currently attempting to synthesize deuterated AA with collaborators to determine the nature of the hydrogen atom abstraction step for 12-hLO.

The nature of the rate-limiting step for 15-hLO, however, can be fully investigated because 15-hLO does oxidize LA. The $^{\text{D}}k_{\text{cat}}$ was temperature-independent which indicates that the rate of product release is solely limited by hydrogen atom abstraction, as previously seen for sLO-1 (26, 36, 44, 46, 51). The magnitude of the $^{\text{D}}k_{\text{cat}}$ was large (40 ± 8), which

indicates a tunneling mechanism for hydrogen atom transfer. Previously, we published a large $^{\text{D}}k_{\text{cat}}/K_{\text{M}}$ for 15-hLO (using a competitive HPLC method) which was temperature-dependent (36). This result is corroborated in the steady-state, noncompetitive KIE study presented here, in which the $^{\text{D}}k_{\text{cat}}/K_{\text{M}}$ was temperature-dependent (Figure 4), and supports our previous hypothesis that there are multiple rate-limiting steps for 15-hLO at low temperatures. These multiple rate-limiting steps effectively lower the magnitude of the observed $^{\text{D}}k_{\text{cat}}/K_{\text{M}}$ at lower temperatures, because the hydrogen atom abstraction, which accounts for the large KIE, is only partially rate limiting and hence only a fraction of the true $^{\text{D}}k_{\text{cat}}/K_{\text{M}}$ value is observed. As the temperature increases, the hydrogen atom abstraction becomes the sole rate-limiting step as seen by the plateau of the $^{\text{D}}k_{\text{cat}}/K_{\text{M}}$ due to the temperature independence of the tunneling mechanism of the abstraction.

The $^{\text{D}}k_{\text{cat}}/K_{\text{M}}$ data clearly indicate the existence of multiple rate-limiting steps at low temperatures; however, more data are needed to determine the nature of these steps. Viscosity experiments were attempted to determine if substrate diffusion is rate-limiting for substrate capture ($k_{\text{cat}}/K_{\text{M}}$); however, no conclusion could be made because all viscogens gave differing results. The SIE was subsequently determined for $k_{\text{cat}}/K_{\text{M}}$ to establish if a solvent-dependent step could be involved as an additional rate-limiting step (Figure 6). A significant $k_{\text{cat}}/K_{\text{M}}$ SIE (2.02 ± 0.02) for 15-hLO was seen at 15 °C, which diminishes as the temperature increases, demonstrating a solvent-dependent rate-limiting step. The k_{cat} SIE, however, was close to unity and temperature-independent, indicating that solvent-dependent steps are not rate-limiting for product release (k_{cat}). Both of these results were in complete agreement with the KIE results and conclusively establish a solvent-dependent step as one of the additional rate-limiting step in the substrate capture ($k_{\text{cat}}/K_{\text{M}}$) at low temperatures. The data also demonstrate that the rate of product release (k_{cat}) is solely limited by hydrogen atom abstraction for 15-hLO.

These results were especially interesting because they mirror the results of sLO-1, where substrate capture ($k_{\text{cat}}/K_{\text{M}}$) displays multiple rate-limiting steps but product release (k_{cat}) does not, suggesting similar molecular mechanisms for

the two enzymes. We previously demonstrated that the catalytic efficiency of sLO-1 was lowered by disruption of the hydrogen bond network that connects the substrate cavity to the iron coordination (Gln₄₉₅, Gln₆₉₇, and Asn₆₉₄) (Figure 7a) (23). We proposed that the hydrogen bond network allowed the substrate binding to affect reactivity by directly changing the coordination distance of Asn₆₉₄ and hence the reactivity of the iron. This hypothesis is corroborated by the sLO-3–HPOD crystal structure, where the position of Gln₅₁₄ (Gln₄₉₅ in sLO-1) is greatly altered by interaction with the bound HPOD (30). This hydrogen bond network is also present in 15-rLO [Glu₃₅₇, Gln₅₄₈, and His₅₄₄ (Figure 7b)] and 15-hLO (sequence ≈80% homologous to that of 15-rLO) (52), which could account for the positive SIE results seen in this investigation of 15-hLO. However, there are differences between the two hydrogen bond networks of 15-hLO/15-rLO and sLO-1, which complicates their comparison. His₅₄₄ of 15-hLO and His₅₄₅ of 15-rLO do not change their coordination distance upon substrate binding, as seen by MCD spectroscopy for Asn₆₉₄ of sLO-1 (53). The hydrogen bond network in 15-rLO, however, could affect the orientation of the His₅₄₅ ligation by its hydrogen bond to Glu₃₅₇ (Figure 7b) (His₅₄₄ and Glu₃₅₆ in 15-hLO, by sequence alignment). This ligation change could modulate the reactivity of the Fe(III)–OH species due to ligand orbital overlap of His₅₄₄ (15-hLO) or His₅₄₅ (15-rLO) with the iron.

This hypothesis that hydrogen bond rearrangement is a rate-limiting step for 15-hLO is surprising since its k_{cat} is 29-fold slower than that of sLO-1, which could potentially make the abstraction step the sole rate-limiting step on $k_{\text{cat}}/K_{\text{M}}$. That this is not the case leads to the intriguing hypothesis that the hydrogen bond rearrangement step is chemically linked with the hydrogen atom abstraction step and hence could constitute a conserved mechanism for both 15-hLO and sLO-1. This requires further investigation of the second coordination sphere of 15-hLO, and specific mutations are currently being investigated.

In addition to confirming that 15-hLO has multiple rate-limiting steps with regard to substrate capture ($k_{\text{cat}}/K_{\text{M}}$), these KIE experiments have also allowed us to address the nature of the tunneling mechanism of hydrogen atom abstraction. Knapp and Klinman have recently proposed a hydrogen atom transfer promoted by environmental vibrations to explain the large kinetic isotope effects in sLO-1 (24, 54, 55). These vibrations are termed “active dynamics” and are responsible for the gating which promotes hydrogen transfer. If we compare the 15-hLO k_{cat} temperature dependence with that of sLO-1, we observe significant differences (Table 2). The magnitude of Dk_{cat} has decreased for 15-hLO from that of sLO-1 (40 vs 81); the E_{act} has increased (7.7 vs 2.1), and the $A_{\text{H}}/A_{\text{D}}$ has decreased (8 vs 18). These combined results are consistent with the hypothesis that the hydrogen transfer coordinate for 15-hLO has a greater gating component than that of sLO-1 and suggests a less constricted binding site, as previously seen for sLO-1 active site mutants (24). This conclusion is consistent with the fact that 15-hLO has evolved to catalyze AA, not LA, and thus, a greater gating component could be introduced to the hydrogen atom transfer for LA. This gating hypothesis can be tested by comparing the kinetics of deuterated AA with those of deuterated LA and is currently under investigation in conjunction with a collaborator’s lab.

To summarize, human lipoxygenases have appeared to retain a high rate of substrate capture [$k_{\text{cat}}/K_{\text{M}}$ and $k_{\text{cat}}/K_{\text{M(O}_2\text{)}}$] such that these rates are comparable to or better than that of sLO-1, at physiological temperature (37 °C). Despite this, their rates of product release (k_{cat}) have slowed relative to that of sLO-1. 12-hLO has an SIE profile distinct from those of 15-hLO and sLO-1, which suggests different microscopic rate-limiting steps. 15-hLO manifests a solvent-dependent rate-limiting step during substrate capture ($k_{\text{cat}}/K_{\text{M}}$), which suggests that sLO-1 and 15-hLO have a common mechanism which links the hydrogen atom abstraction and the hydrogen bond rearrangement. We propose this common mechanism is due to a hydrogen bond rearrangement of the second coordination sphere (Figure 7), which is similar in both sLO-1 and 15-hLO/15-rLO. Finally, 15-hLO displays a decreased Dk_{cat} , an increased E_{act} , and a decreased $A_{\text{H}}/A_{\text{D}}$, which indicates a significant gating component in the hydrogen atom abstraction suggesting a “loose” fit for LA in the active site. Our group is currently exploring this work further using the deuterated, endogenous substrate, AA, with 12-hLO and 15-hLO to address the differences in their microscopic rate constants.

ACKNOWLEDGMENT

We gratefully acknowledge J. Klinman and M. Knapp for the use of the Clark O₂ electrode and their helpful comments in the preparation of the manuscript. We thank C. Funk for the plasmid containing the gene for 12-hLO and S. Whitman for technical support.

REFERENCES

- Porta, H., and Rocha-Sosa, M. (2001) *Microbiology* 147, 3199–3200.
- Gardner, H. W. (1995) *Hortic. Sci.* 30, 197–205.
- Grechkin, A. (1998) *Prog. Lipid Res.* 37, 317–352.
- Brash, A. R. (1999) *J. Biol. Chem.* 274, 23679–23682.
- Gardner, H. W. (1991) *Biochim. Biophys. Acta* 1084, 221–239.
- Siedow, J. N. (1991) *Annu. Rev. Plant Physiol. Plant Mol. Biol.* 42, 145–188.
- Samuelsson, B., Dahlen, S. E., Lindgren, J. A., Rouzer, C. A., and Serhan, C. N. (1987) *Science* 237, 1171–1176.
- Sigal, E. (1991) *J. Am. Phys. Soc.* 260, 13–28.
- Steele, V. E., Holmes, C. A., Hawk, E. T., Kopelovich, L., Lubet, R. A., Crowell, J. A., Sigman, C. C., and Kelloff, G. J. (1999) *Cancer Epidemiol., Biomarkers Prev.* 8, 467–483.
- Dailey, L. A., and Imming, P. (1999) *Curr. Med. Chem.* 6, 389–398.
- Nakano, H., Inoue, T., Kawasaki, N., Miyataka, H., Matsumoto, H., Taguchi, T., Inagaki, N., Nagai, H., and Satoh, T. (2000) *Bioorg. Med. Chem.* 8, 373–380.
- Gosh, J., and Myers, C. E. (1998) *Proc. Natl. Acad. Sci. U.S.A.* 95, 13182–13187.
- Hussain, H., Shornick, L. P., Shannon, V. R., Wilson, J. D., Funk, C. D., Pentland, A. P., and Holtzman, M. J. (1994) *Am. J. Physiol.* 266, C243–C253.
- Connolly, J. M., and Rose, D. P. (1998) *Cancer Lett.* 132, 107–112.
- Natarajan, R., and Nadler, J. (1998) *Front. Biosci.* 3, E81–E88.
- Harats, D., Shaish, A., George, J., Mulkins, M., Kurihara, H., Levkovitz, H., and Sigal, E. (2000) *Arterioscl., Thromb., Vasc. Biol.* 20, 2100–2105.
- Kamitani, H., Geller, M., and Eling, T. (1998) *J. Biol. Chem.* 273, 21569–21577.
- Yamamoto, S. (1992) *Biochim. Biophys. Acta* 1128, 117–131.
- DeGroot, J. J., Veldink, G. A., Vliegenhart, J. F. G., Boldingh, J., Wever, R., and Van Gelder, B. F. (1975) *Biochim. Biophys. Acta* 377, 71–79.
- Ruddat, V. C., Whitman, S., Holman, T. R., and Bernasconi, C. F. (2003) *Biochemistry* 42, 4172–4178.

21. Scarrow, R. C., Trimitsis, M. G., Buck, C. P., Grove, G. N., Cowling, R. A., and Nelson, M. J. (1994) *Biochemistry* 33, 15023–15035.
22. Glickman, M. H., and Klinman, J. P. (1996) *Biochemistry* 35, 12882–12892.
23. Tomchick, D. R., Phan, P., Cymborowski, M., Minor, W., and Holman, T. R. (2001) *Biochemistry* 40, 7509–7517.
24. Knapp, M. J., Rickert, K., and Klinman, J. P. (2002) *J. Am. Chem. Soc.* 124, 3865–3874.
25. Knapp, M., Seebeck, F. P., and Klinman, J. (2001) *J. Am. Chem. Soc.* 123, 2931–2932.
26. Glickman, M. H., and Klinman, J. P. (1995) *Biochemistry* 34, 14077–14092.
27. Northrop, D. B. (1998) *J. Chem. Educ.* 75, 1153–1157.
28. Rickert, K. W., and Klinman, J. P. (1999) *Biochemistry* 38, 12218–12228.
29. Skrzypczak-Jankun, E., Amzel, L. M., Kroa, B. A., and Funk, M. O. (1997) *Proteins* 29, 15–31.
30. Skrzypczak-Jankun, E., Bross, R. A., Carroll, R. T., Dunham, W. R., and Funk, M. O. (2001) *J. Am. Chem. Soc.* 123, 10814–10820.
31. Boyington, J. C., Gaffney, B. J., and Amzel, L. M. (1993) *Biochem. Soc. Trans.* 21, 744–748.
32. Minor, W., Steczko, J., Bolin, J. T., Otwinowski, Z., and Axelrod, B. (1993) *Biochemistry* 32, 6320–6323.
33. Minor, W., Steczko, J., Boguslaw, S., Otwinowski, Z., Bolin, J. T., Walter, R., and Axelrod, B. (1996) *Biochemistry* 35, 10687–10701.
34. Prigge, S. T., Boyington, J. C., Gaffney, B. J., and Amzel, L. M. (1996) *Proteins* 24, 275–291.
35. Gillmor, S. A., Villasenor, A., Fletterick, R., Sigal, E., and Browner, M. (1997) *Nat. Struct. Biol.* 4, 1003–1009.
36. Lewis, E. R., Johansen, E., and Holman, T. R. (1999) *J. Am. Chem. Soc.* 121, 1395–1396.
37. Holman, T. R., Zhou, J., and Solomon, E. I. (1998) *J. Am. Chem. Soc.* 120, 12564–12572.
38. Mogul, R., Johansen, E., and Holman, T. R. (2000) *Biochemistry* 39, 4801–4807.
39. Amagata, T., Whitman, S., Johnson, T., Stessmann, C. C., Carroll, J., Loo, C., Clardy, J., Lobkovsky, E., Crews, P., and Holman, T. R. (2003) *J. Nat. Prod.* 66, 230–235.
40. Mogul, R., and Holman, T. R. (2001) *Biochemistry* 40, 4391–4397.
41. Chen, X.-S., Brash, A. R., and Funk, C. D. (1993) *Eur. J. Biochem.* 214, 845–852.
42. Kuhn, H., Barnett, J., Grunberger, D., Baecker, P., Chow, J., Nguyen, B., Bursztynpettegrew, H., Chan, H., and Sigal, E. (1993) *Biochim. Biophys. Acta* 1169, 80–89.
43. Gan, Q. F., Witkop, G. L., Sloane, D. L., Straub, K. M., and Sigal, E. (1995) *Biochemistry* 34, 7069–7079.
44. Glickman, M. H., Wiseman, J. S., and Klinman, J. P. (1994) *J. Am. Chem. Soc.* 116, 793–794.
45. Sigal, E., Grunberger, D., Craik, C. S., Caughey, G. H., and Nadel, J. A. (1988) *J. Biol. Chem.* 263, 5328–5332.
46. Jonsson, T., Glickman, M. H., Sun, S. J., and Klinman, J. P. (1996) *J. Am. Chem. Soc.* 118, 10319–10320.
47. Rapoport, S. M., Hartel, B., and Hausdorf, G. (1984) *Eur. J. Biochem.* 139, 573–576.
48. Kuhn, H., Walther, M., and Kuban, R. J. (2002) *Prostaglandins Other Lipid Mediators* 68–69, 263–290.
49. Jones, D. P. (1986) *Am. J. Physiol.* 250, C663–C675.
50. Albery, W. J., and Knowles, J. R. (1976) *Biochemistry* 15, 5631–5640.
51. Hwang, C. C., and Grissom, C. B. (1994) *J. Am. Chem. Soc.* 116, 795–796.
52. Sigal, E., Grunberger, D., Highland, E., Gross, C., Dixon, R. A. F., and Craik, C. S. (1990) *J. Biol. Chem.* 265, 5113–5120.
53. Solomon, E. I., Zhou, J., Neese, F., and Pavel, E. G. (1997) *Chem. Biol.* 4, 795–808.
54. Knapp, M. J., and Klinman, J. P. (2002) *Eur. J. Biochem.* 269, 3113–3121.
55. Kuznetsov, A. M., and Ulstrup, J. (1999) *Can. J. Chem.* 77, 1085–1096.

BI0273462